

On the topology of microlensing events of Earth-Sun fraction mass systems

L. de Almeida¹ & J.-D. Jr. do Nascimento¹

¹ Federal University of Rio Grande do Norte, Natal, RN, Brazil e-mail: dealmeida.l@fisica.ufrn.br

Abstract. In this work, we analyze the topology of microlensing events that generate light curves in which it would be possible to detect Earth-mass planets around Solar-mass stars. We used the semi-analytical method of solving the lens equation to generate light curves and compare them with pre-defined synthetic models by varying all the parameters of the event. We propose the parametrization of two of these parameters: the smallest apparent distance between the source star and the lens (impact parameter μ_0); and the angle between the source path and the lens system arbitrary axis (impact angle α). Our parametrization aims to force the path of the source to pass through the region of interest of the event, thus increasing the probability of detection of a low mass planet. We focused on simulating systems with mass fraction and semi-major axis similar to the Sun-Earth system.

Resumo. Neste trabalho, nós analisamos a topologia de eventos de microlentes gravitacionais que produzem curvas de luz em que a detecção de planetas com a massa similar à da Terra é possível. Usamos o método semi-analítico de resolução da equação da lente para gerar curvas de luz e compara-las com modelos sintéticos pré-definidos, variando todos os parâmetros do evento. Propomos a parametrização de dois desses parâmetros: a menor distância entre o trajeto da estrela fonte e a lente principal (parâmetro de impacto μ_0); e o ângulo que o caminho da fonte faz com o eixo relativo do sistema (ângulo de impacto α). Nossa parametrização força o caminho da fonte a passar pela região de interesse do evento em que seria possível a detecção de planetas de baixa massa, aumentando a probabilidade de detecção de planetas com a massa da Terra. Nos focamos em simular sistemas com a fração de massa e semi-eixo maior similares ao sistema Sol-Terra. Apresentamos as topologias e as implicações da nossa parametrização na busca por planetas em eventos de microlentes gravitacionais.

Keywords. Gravitational lensing: micro – Planets and satellites: detection – Methods: data analysis.

1. Introduction

In the last decade, the number of discovered exoplanets has grown exponentially, mainly due to the detections from the transit and radial velocity techniques. These discoveries show us that, giant planets orbiting very close to their stars, are the common types of exoplanets to be discovered. In contrast, the gravitational microlensing technique has the sensitivity to detect low-mass planets in orbits from 0.5 to 10 AU Gould et al. (2014). Because it depends only on the combined gravitational field of the star-planet, this technique can detect planets in faint stars, which would be difficult for other techniques that depends on the star's light. The observational surveys Microlensing Planet Search (MPS) (Rhie 1999) and Microlensing Observations in Astrophysics (MOA) (Rhie et al. 2000; Sumi et al. 2003) demonstrated for the first time that sensibility and even showed the capability of microlensing technique to discover Earth-mass planets around 1AU in binary systems. As discussed by Albrow et al. (2001); Gaudi et al. (2002), more than 77% of exoplanetary systems discovered with microlensing techniques shows planets with masses lower than Jupiter mass and with semi-major axis between 1.5 and 4 AU. These results are consistent with the fact that massive planets far away from their central stars are easier to be detected with microlensing method (Sumi et al 2006; Han 2006). In this context, (Paczynski 1986) shows that detection is function of the impact parameter μ_0 and the impact angle α . Here, in this study we propose a parametrization of the source's path to force it to cross the Caustic Region Of Interest (CROIN) (Penny 2014). This give advantage to the detections of Earth-like planets around Solar-like stars by microlensing events. We explore the caustic topology for events with a semi-major axis of about 1AU and with the lens at half

distance away from the center of our galaxy. We present light curves where it is possible conducted an analysis of the μ_0 and α variation as a function of fixed parameters in the lens-planet apparent separation. We constructed a model to simulate our system based on a semi-analytical method for solving the binary lens equation take into account the source, lenses, caustic and critic curves. We used part of this approach to obtain the results published in Almeida & do Nascimento (2018).

2. The microlensing event

A gravitational microlensing event occurs when a star in the foreground (lens) passes near the line of sight of a background star (source) and get their light bend from the original path. This bending of the light generates a relative magnification of the source and if the system source-lens have relative movements, a characteristic light curve is produced. The deflection of the light by a single star can be express by $\alpha = \frac{4GM}{c^2 r}$, where α is the deflection angle, M é the lens mass, G is the universal gravitational constant, c is the speed of light and r is the apparent distance between the source and the lens. If we establish D_S as the distance between the observer and the source and D_L as the distance between the observer and the lens, we can write the distance between the source and lens as $(D_S - D_L)$, and we can derive the well know equation of the Einstein Radius

$$\theta_E = \sqrt{\frac{4GM}{c^2} \frac{D_S - D_L}{D_L - D_S}}. \quad (1)$$

The Eq. 1 holds for sources and lens that are aligned. Introducing the small distance β between the source and the lens, we can derive the lens equation for the single lens case

as $\beta = \theta - \frac{\theta_E^2}{\theta}$ which is the well known lens equation for the single lens case, and it can be easily solved as a second degree polynomial.

2.1. Formalism

For the 2 lenses case, we can rewrite β , originally written for single lens case, in cartesian coordinates and multiple lenses as

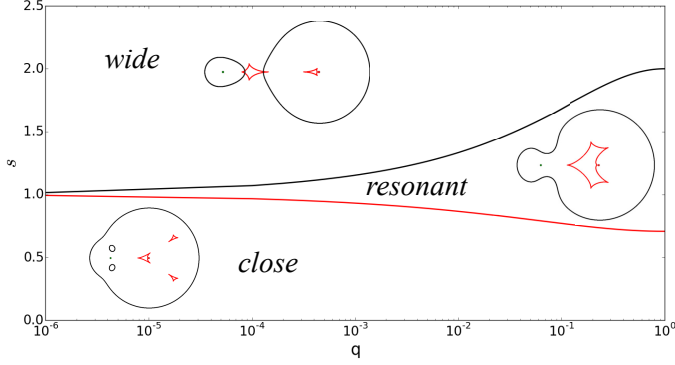


FIGURE 1. Different topologies dependent on s and q .

$$x_s = x - \sum \frac{m_i(x - x_i)}{(x - x_i)^2 + (y - y_i)^2}, \quad (2)$$

$$y_s = y - \sum \frac{m_i(y - y_i)}{(x - x_i)^2 + (y - y_i)^2}, \quad (3)$$

where m_i is the i th mass fraction of the i th lens of the system. x_s and y_s are the cartesian positions of the source. x_i and y_i are the lens position of the i th lens. Here we are using the complex notation to denote the lens equation for the two lenses (Witt H. J 1990; Witt & Mao 1995) case, representing a host star and their planet as

$$\omega = z - \frac{\varepsilon_1}{\bar{z} + \bar{z}_1} - \frac{\varepsilon_2}{\bar{z} + \bar{z}_2}. \quad (4)$$

In the above equation, ε_1 and ε_2 are the lenses masses, with $\varepsilon_1 + \varepsilon_2 = 1$. The parameter z is the images positions complex solutions set. The ω is the relative position of the source at a specific time. \bar{z}_1 and \bar{z}_2 are the lenses positions complex conjugate.

2.2. The semi-analytic method

Technically, to solve a lens equation with $n = 2$, it is necessary to invert a 5th order polynomial and solve it to find the polynomial roots. To accomplish this task we developed a model that uses a semi-analytic method to find polynomial coefficients and solutions (Witt H. J 1990). For the case where the source is not close enough to the caustic-crossing region, we used the point source magnification method to solve and obtain the light curve. In this case, the point source magnification uses the Jacobian determinant give by

$$J = \frac{\partial \omega}{\partial z} \frac{\partial \bar{\omega}}{\partial \bar{z}} - \frac{\partial \omega}{\partial \bar{z}} \frac{\partial \bar{\omega}}{\partial z} = 1 - \left| \frac{\partial \omega}{\partial \bar{z}} \right|^2, \quad (5)$$

where

$$\frac{\partial \omega}{\partial \bar{z}} = \frac{\varepsilon_1}{(\bar{z} + \bar{z}_1)^2} - \frac{\varepsilon_2}{(\bar{z} + \bar{z}_2)^2}. \quad (6)$$

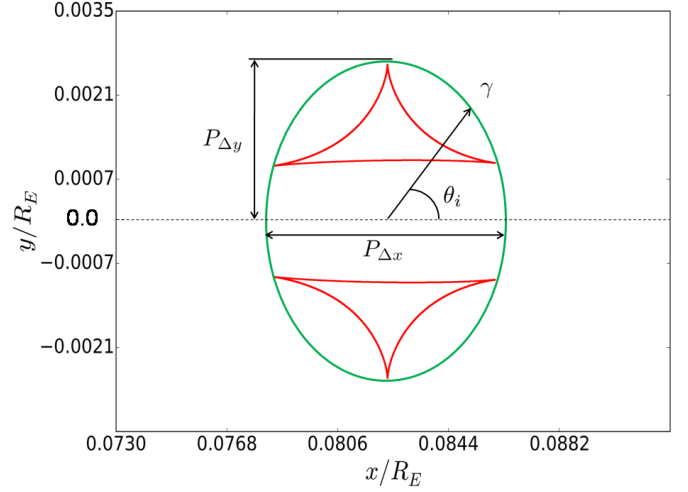


FIGURE 2. Planetary caustic in detail with $q = 3.003467 \times 10^{-6}$, $s = 0.9597E_R$, $\mu_0 = 0.0082E_R$. The green ellipse is the influence area defined by the Eq. 14

The Jacobian gives us the ratio between a given transformation and its original basis. Thus, To determine a relation between the images and their source, we need to compute the inverse of the Jacobian as $A = \frac{1}{|J|}$.

3. Earth-mass like systems topology

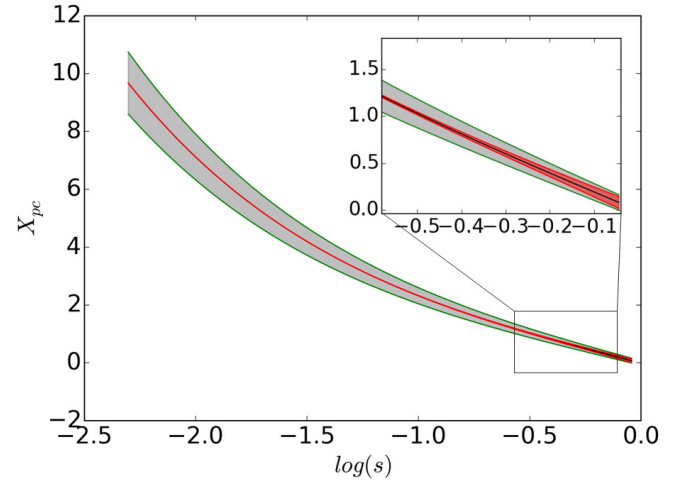


FIGURE 3. Plot of X_{pc} dependent on $\log s$ for our wanted system with $q = 3.003467 \times 10^{-6}$ and $0.95969 > s > 0.1$. The gray region is $2P_{\Delta y}$ and the red region is $P_{\Delta x}$ (both times by 20 for better visualization)

Caustics modeling and microlensing critical event curves depends fundamentally on the apparent semi-major axis s between the lenses, i.e., the host lens and the planet. Here we used Einstein radius units R_E , and the mass fraction as $q = M_2/M_1$, where M_2 stands for the planet mass and M_1 for the host star mass, and by definition $M_1 + M_2 = 1$. The source's path is defined by 2 parameters, the impact parameter μ_0 and the impact angle α . The impact parameter μ_0 represents the closest distance between the source and the host lens at the time t_0 .

In general, binary systems caustics produce topology close, resonant and wide (Schneider & Weiss 1987; Erdl & Schneider

1993), and with limits varying as a function of s and q , as shown in the Fig. 1. For this case, the impact angle α is the angle between the source trajectory and the x -axis of the system. For the 2 lenses case, the system lies in the x -axis.

For systems like our Sun-Earth system, in terms of Earth-Sun mass ratio, we find $q = 3 \times 10^{-6}$ and $s = 0.95969$, whereas the $M_1 = M_\odot$ and $1R_E = 1.0420AU$. In such a system, a planet orbiting a major-semi axis of $1AU$ it would lie at the Einstein Ring limit. Nevertheless, we cannot ignore possible values of $s < 1AU$ due to the fact that for this systems the major-semi axis is the projected separation between the planet and its host star. By considering systems with $q = 3 \times 10^{-6}$ and s independent, only two topologies can be obtained, they are wide or close. As presented by (Erdl & Schneider 1993), systems with such a wide topology satisfy the condition

$$s > \sqrt{\frac{(1+q^{\frac{1}{3}})^3}{1+q}}. \quad (7)$$

For the interval $0.1R_E < s < 0.95969$, our system can only be closed. Thus, to adjust the μ_0 and α parameters in an efficient way, we need to know the position of the planetary caustic as a function of the s variation.

By analyzing the Fig. 1, we can conclude that a system with an Earth-Sun mass ratio can only be within a wide topology if $s > 1.0217R_E$. On the other hand, as our system can only assume $0.1R_E < s < 0.95969$, we can discard the wide topology for systems like our own. Thus, to use microlensing path parametrization for Earth-like exoplanet detections around solar mass stars it is necessary a deep analysis of the close topology case.

3.1. Closed topology case

The closed topology is formed by three caustics. A central caustic close to the primary lens and two identical planetary caustics on the system axis and opposite side of the planet. For a light curve of a source that passes close the central caustic and on the same side as the planet, we will only detect the main lens signature. Following results from Erdl & Schneider (1993), we can define the topology system as closed when the condition below is satisfied

$$\frac{q}{(1+q)^2} < s^{-8} \left(\frac{1-s^4}{3} \right)^3. \quad (8)$$

In the above equation, for $q = 3 \times 10^{-6}$, a system like our Sun-Earth system can only be close if $s < 0.9893$. In order to set the region of influence, we need at this point, to define the planetary caustic characteristics for closed systems. Considering x as the position of the planetary caustic, that can be determined through the following equation (Han 2006)

$$X_{pc} = \frac{1}{1+q} \left(s - \frac{1-q}{s} \right), \quad (9)$$

where X_{pc} is the separation between primary lens and the center of the planetary caustic. The Eq. 9 makes clear that the smaller s , the larger the value of X_{pc} . By using this position X_{pc} we were able to parametrize some geometrical proprieties of the system and also to set the dependency of the source's path with the localization of the influence region around the planetary caustic. We can also link the position X_{pc} of the planetary caustic center with the impact parameter μ_0 by the following equation

$$\mu_0 = \frac{|s^2 + q - 1| \cdot |\tan(\alpha)|}{|q + 1| \cdot |s| \cdot \sqrt{\tan(\alpha)^2 + 1}}. \quad (10)$$

To better describe the entire region of interest we need to described geometrically the entire area containing the planetary caustic. For that, following the geometry of the problem, we found values for $P_{\Delta x}$ and $P_{\Delta y}$, (Fig. 2) written below

$$P_{\Delta x} = \frac{3}{2} s^3 \sqrt{3} \sqrt{q}, \quad (11)$$

$$P_{\Delta y} = 2 \frac{\sqrt{q}}{s \sqrt{s^2 + 1}}. \quad (12)$$

The size of the influence area, which contains the planetary caustic, can be defined through an ellipse area πab , with $a = P_{\Delta x}/2$ and $b = P_{\Delta y}$. Thus, the influence area that defines the region containing the planetary caustic is

$$A = \pi \frac{P_{\Delta x}}{2} P_{\Delta y}. \quad (13)$$

Entering the Eqs. 11 and 12 into the Eq. 13, we determined the area size A that contains the planetary caustic as presented by the green ellipse in the Fig. 2, and now as a function of q and s

$$A = \frac{\gamma^2 \pi s^2 \sqrt{3} q}{\sqrt{s^2 + 1}}, \quad (14)$$

where γ is a scalar factor for the size of the area which contains the planetary caustic. For the particular case of γ equal to 1, Fig. 2, such area fits perfectly the planetary caustic.

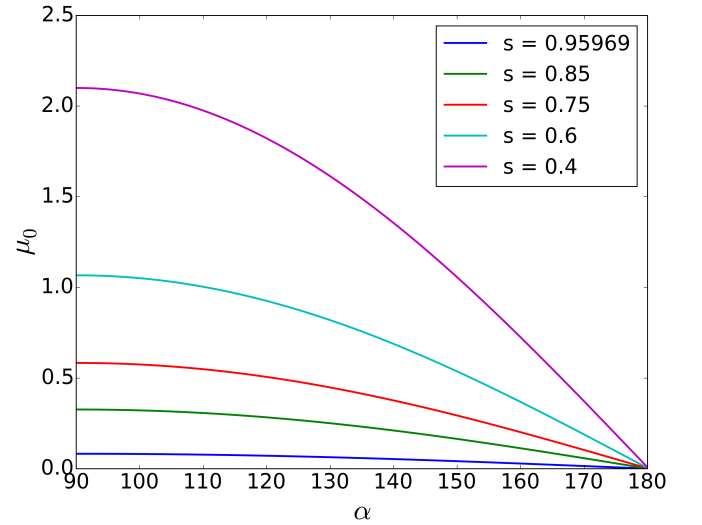


FIGURE 4. Evolution of the impact angle α when different initial μ_0 is set for $s = 0.95969, 0.85, 0.75, 0.6$ e 0.4 .

By analyzing the Fig. 3 we find that, for systems with close topology, the distance X_{pc} increases as s decreases. We can also see, based on Eqs. 11 and 12, that $P_{\Delta x}$ drastically decreases and $P_{\Delta y}$ increase when s approaches the origin. The Eq. 14 leads to the conclusion that the area of the planetary caustic overall decreases when s approaches the origin. Thus, even with X_{pc} getting bigger when s decreases, the total area it is not enough for any possible detection. The Fig. 3 leads to the conclusion that $2P_{\Delta y}$ and $P_{\Delta x}$ approaches to the same value when s approaches to 1.

To link the source path with the *Caustic Region Of Influence* (CROIN)(Penny 2014), we define all the points on the ellipse using the Eqs. 11 and 12 as

$$X_{ip} = \gamma P_{\Delta x} \cos(\theta_i) + X_{pc}, \quad (15)$$

$$Y_{ip} = \gamma P_{\Delta y} \sin(\theta_i). \quad (16)$$

If we evolve θ_i from 0 to 2π in the equations above, we define the perimeter of the ellipse of area A , for the close topology case. Now, we can define the parameterization of the source path to the close topology case by the next equation

$$\mu_i = \frac{|\tan(\alpha)X_{ip} - Y_{ip}|}{\sqrt{\tan(\alpha)^2 + 1}}. \quad (17)$$

By setting $\gamma = 1$, and varying α from 0 to 2π , we got all values of μ_0 from the Eq. 17 with the path of the source always passing by the planetary caustic vicinity. Thus, to explore all the possible light curves for our Earth-Sun model, we need to vary γ , α and θ_i .

Fig. 4 presents the evolution of the impact angle α when different initial μ_0 is set to $s = 0.95969, 0.85, 0.75, 0.6$ and 0.4 . We can see in all cases that the impact parameter μ_0 must be smaller than the position of the planetary caustic or else the path of the source will not pass through the region of influence.

From the Fig. 4 and relative Eq. 10 we see that, as α approaches 90 (perpendicular to the lens axis) the value of μ_0 increases. That happens because, in order to the source's path to cross the interest region in X_{pc} , μ_0 need to be 0 so that $\alpha = 2\pi$ and if the path is perpendicular, with $\alpha = \pi/2$, then μ_0 must be set to the value of X_{pc} .

4. SUMMARY AND DISCUSSION

We analyzed a set of simulations constructed to search Earth-like exoplanet around solar mass stars. Our simulations involved a parameter search on Sun-Earth models created using the semi-analytical method.

We find that all solutions involving closed topologies are not degenerated and since we are searching only around the region of interest, computationally, the speed-up factor depends directly on the fraction between the R_E area and the area that contains the planetary caustic from Eq. 14. For a system with mass fraction and semi-major axis apparent similar to our Sun-Earth system and $t_E = 90$ days, we find that the planetary deviation takes about 1 day and can be observed by high cadence surveys, such as LSST (first light planned to 2019) and WFIRST (planned to be launched in 2024). We find that Sun-Earth analogue observed system will present a close topology (for semi-major axis close to 1 AU) with doubled identical caustics on the other side of the planet. We also concluded that the ellipse around the planetary caustic decreases exponentially as s increases. We find that if the semi-major axis is equal to 1 AU, then the deviation of the light curve from the single-lens case will last for about one day (for $t_E = 90$ days). The new values for X_{ip} and Y_{ip} are implemented within the new parametrization of $\alpha(\mu_0)$ and can easily be integrated in the parameters search with γ dictating the evolution of α once we have defined a fixed μ_0 .

Acknowledgements. We thank the University of Rio Grande do Norte and CAPES for the financial support.

References

- Albrow, M. D., et al. 2001, Limits on the Abundance of Galactic Planets From 5 Years of PLANET Observations, *Astrophys. J. Lett.*, 556, L113
- Alcock, C., Allsman, R. A., Axelrod, T. S., et al. 1995, *Physical Review Letters*, 74, 2867
- L. de Almeida & J.-D. Jr. do Nascimento, 2018, submitted, Microlensing path parametrization for Earth-like Exoplanet detections around Solar mass Stars.
- Bennett, D. P., & Rhie, S. H. 1996, *apj*, 472, 660
- Bozza, V. 2000, *aap*, 359, 1
- Einstein, A. 1936, *Science*, 84, 506
- Erdl, H., & Schneider, P. 1993, *aap*, 268, 453
- Gaudi, B. S., et al. 2002, Microlensing Constraints on the Frequency of Jupiter-Mass Companions: Analysis of 5 Years of PLANET Photometry, *Astrophys. J.*, 566, 463
- Gould, A., Udalski, A., Shin, I.-G., et al. 2014, *Science*, 345, 46
- Griest, K., Lehner, M. J., Cieplak, A. M., & Jain, B. 2011, *Physical Review Letters*, 107, 231101
- Hamadache, C., Le Guillou, L., Tisserand, P., et al. 2006, *aap*, 454, 185
- Han, C., Gould, A. 1995, *ApJ*, 447, 53
- Han, C. 2006, *ApJ*, 638, 1080
- Liebes, S. 1964, *Physical Review*, 133, 835
- Mao, S., & Paczynski, B. 1991, *apjl*, 374, L37
- Paczynski, B. 1986, *ApJ*, 304, 1
- Penny, M. T. 2014, *apj*, 790, 142
- Rhie, S. H. 1999, *arXiv:astro-ph/9909433*
- Rhie, S. H. et al. 2000, On Planetary Companions to the MACHO 98-BLG-35 Microlens Star, *Astrophys. J.*, 533, 378
- Schneider, P., & Weiss, A. 1987, *aap*, 171, 49
- Sumi, T., Abe, F., Bond, I. A., et al. 2003, *ApJ*, 591, 204
- Sumi, T., et al. 2006, Microlensing Optical Depth toward the Galactic Bulge Using Bright Sources from OGLE-II, *Astrophys. J.*, 636, 240
- Witt H. J., 1990, *Astronomy and Astrophysics (ISSN 0004-6361)*
- Witt, J., Mao, S., 1995, *ApJ*, 447, 105